Structural and Guanosine Triphosphate/Diphosphate Requirements for Transit Peptide Recognition by the Cytosolic Domain of the Chloroplast Outer Envelope Receptor, Toc34[†]

E. Schleiff,*[,‡] J. Soll,[‡] N. Sveshnikova,[‡] R. Tien,[‡] S. Wright,[§] C. Dabney-Smith,[§] C. Subramanian,[||] and B. D. Bruce*[,§,⊥]

Institut of Botany, University Kiel, Am Botanischen Garten 1-9, 24118 Kiel, Germany, and Department of Biochemistry and Cellular & Molecular Biology, Graduate Program in Plant Physiology and Genetics, and Center of Excellence in Structural Biology, University of Tennessee, Knoxville, Tennessee 37996

Received June 28, 2001; Revised Manuscript Received October 26, 2001

ABSTRACT: Toc34 is a transmembrane protein located in the outer envelope membrane of chloroplasts and involved in transit peptide recognition. The cytosolic region of Toc34 reveals 34% α-helical and 26% *β*-strand structure and is stabilized by intramolecular electrostatic interaction. Toc34 binds both chloroplast preproteins and isolated transit peptides in a guanosine triphosphate- (GTP-) dependent mechanism. In this study we demonstrate that the soluble, cytosolic domain of Toc34 (Toc34ΔTM) functions as receptor in vitro and is capable to compete with the import of the preprotein of the small subunit (preSSU) of ribulose-1,5-bisphosphate carboxylase−oxygenase into chloroplasts in a GTP-dependent manner. We have developed a biosensor assay to study the interaction of Toc34ΔTM with purified preproteins and transit peptides. The results are compared with the interactions of both a full-size preprotein and the transit peptide of preSSU with the translocon of the outer envelope of chloroplasts (Toc complex) in situ. Several mutants of the transit peptide of preSSU were evaluated to identify amino acid segments that are specifically recognized by Toc34. We present a model of how Toc34 may recognize the transit peptide and discuss how this interaction may facilitate interaction and translocation of preproteins via the Toc complex in vivo.

Translocation of proteins across the membranes of the endosymbiotically derived organelles such as plastids and mitochondria is facilitated by translocation machines known as translocons (*1*, *2*). The translocon localized in the envelope membranes of the chloroplasts comprises the translocon at the outer and at the inner envelope membranes of chloroplasts, named Toc and Tic[1] (*3*). The initial step of translocation is the recognition of the preprotein by receptors. Subsequently translocation across the membrane through the translocation channel Toc75 occurs (*4*, *5*). Two proteins localized in the outer envelope are identified as receptor proteins, namely, Toc34 and Toc159. Both proteins can be phosphorylated and bind GTP (*6*−*8*). Phosphorylation of Toc34 abolished its interaction with preSSU (*7*), suggesting that the active receptor in vivo is not phosphorylated. The ability of Toc34 and Toc159 to recognize the preproteins has been shown to be positively influenced by the addition of GTP (*7*, *9*, *10*). Furthermore, the addition, prior to binding, of an excess of a C-terminal truncated form of *Arabidopsis thaliana* Toc33 (atToc33), a developmental isoform of Toc34, reduces the binding of a wheat germ-translated form of preSSU to the surface of spinach chloroplasts in vitro (*11*). This interaction was GTP-dependent and suggested that atToc33 is involved specifically in the binding/import of preSSU into chloroplasts (*11*). Indeed, it was demonstrated in a reconstituted system that Toc34 from *Pisum sativum* interacts directly with preSSU (*7*).

For most plastid and mitochondrial preproteins, receptor recognition is mediated by a targeting signal found within the N-terminal extensions known as transit peptides or presequences, respectively. (*12*−*14*). These signals are both necessary and sufficient to initiate translocation in a post-translational process (*15*, *16*). The targeting signals show no obvious blocks of conserved amino acid sequence (*13*,

[†] This work was supported by grants from "The Human Frontiers Science Programme", the Deutsche Forschungsgesellschaft, and the Fonds der Chemischen Industrie to J.S. and by a grant from the Cell Biology Program at NSF to B.D.B. B.D.B. was also supported by a SARIF travel award.

* Corresponding author: Phone 0049-431-880-4213; fax 0049-431-880-4222; e-mail eschleiff@bot.uni-kiel.de.

[‡] University Kiel.

[§] Department of Biochemistry and Cellular & Molecular Biology, University of Tennessee.

[||] Graduate Program in Plant Physiology and Genetics, University of Tennessee.

[⊥] Center of Excellence in Structural Biology, University of Tennessee.

[1] Abbreviations: NTA, nitrilotriacetic acid; SSU, small subunit of ribulose-1,5-bisphosphate carboxylase−oxygenase (Rubisco); preSSU and mSSU, preprotein and mature forms of the small subunit of ribulose-1,5-bisphosphate carboxylase−oxygenase; preFd, preprotein form of ferredoxin; preOE23/33, preprotein form of the 23/33 kDa subunit of the oxygen-evolving complex; Tic/Toc, translocon on the outer/inner envelope of chloroplast; Toc34ΔTM, cytosolic domain of the 34 kDa subunit of the Toc complex.

10.1021/bi011361+ CCC: $22.00
Published on Web 01/17/2002

14). Instead, common secondary or tertiary structural elements are thought to enable the functionality of the targeting sequences. Unfortunately, the details of these structural elements are still largely unknown.

Both mitochondrial and chloroplast targeting signals have been shown to form amphipathic α-helices in membrane-mimetic environments (*17*−*19*). Within mitochondrial presequences the helicity is often broken by a central flexible linker region (*20*). This flexible region is important for early recognition by receptor components (*21*) and for processing by the matrix processing peptidase (*22*), yet it is not critical for the translocation step (*23*). Recent investigations revealed that mitochondrial targeting signals can become helical after recognition by receptor components (*24*, *25*).

The transit peptides of algae chloroplasts indicate that the helical regions are also terminated by central, helix-disrupting residues (*26*, *27*). NMR analysis of the higher plant transit peptide from *Silene* ferredoxin revealed that the transit peptide was largely unstructured with the propensity to form short helical structures in both the N- and C-termini (residues 10−13 and 30−34, respectively) when inserted into a mixed micelle (*28*). A similar result was observed for the preprotein of the small subunit of Rubisco, preSSU (*29*). These helical domains are interrupted by a central region that is enriched in proline and glycine residues (*14*). Mutations within this region largely abolish in vitro import, suggesting that transit peptide flexibility is an essential trait for the import process (*30*). Deletion of the N-terminal amino acids 6−14 of the transit peptide of preFd also inhibit import both in vitro and in vivo (*30*, *31*), which is consistent with the identification of an Hsp70 recognition domain at the extreme N-terminus of transit peptides (*32*). Furthermore, deletion of the first helical region (Δ6−14) abolishes membrane association, suggesting that this region of the ferredoxin transit peptide may perform two different functions depending on the interacting partners. In contrast, the deletion of the second helix in the preFd transit peptide results only in a reduction of insertion (*30*). The interaction of the transit peptide of preSSU is also modulated by the mature domain. Deletion of the 74 C-terminal amino acids of preSSU drastically reduced both the import of the truncated preprotein and its ability to competitively inhibit the import of wt preSSU (*33*). Despite this recent progress, nothing is known about the structural requirements for recognition of preproteins or transit peptides by the outer envelope translocation receptors, Toc34 and Toc159.

To elucidate the essential structural and functional features of chloroplast transit peptides that provide maximum organelle specificity during binding and/or translocation, the interaction of transit peptides and mutants and the receptor component Toc34 was studied. We used a truncated, heterologously expressed form of psToc34 to investigate the requirements for its transit peptide recognition. The secondary structure was analyzed by CD, fluorescence, and absorption spectroscopy and chemical denaturation. It provided initial information on how the isolated cytosolic domain is folded in relation to other well-characterized GTPases. Using a sensitive biosensor assay we demonstrated the interaction of psToc34ΔTM and several chloroplast preproteins (preSSU, preOE33, and preOE23). We also investigated the interaction between psToc34ΔTM and synthetic peptides corresponding to the preSSU transit peptide. Finally, the interaction of Toc34 and different transit sequences as well as several mutants of preSSU was investigated to identify regions essential for import and receptor recognition.

MATERIALS AND METHODS

Materials. The bacterial strains BL21-DE3 and NovaBlue (DE3) were obtained from Stratagene, and the vectors pET21d and pET23d were from Novagen. All other chemicals used were purchased from Roth (Karlsruhe, Germany) or Sigma (Munich, Germany).

Generation of PreSSU Site-Directed and C-Terminal Deletion Mutants. The full-length preprotein was subcloned into the *Bam*HI and *Nco*I sites of pET23d (*33*). Mutations were introduced by long-distance polymerase chain reaction with primers containing the desired codon changes. The parental DNA was then digested with *Dpn*I, which cleaves only methylated DNA. The product was used to transform NovaBlue (DE3) supercompetent cells. Plasmid DNA was isolated and sequenced in both directions to confirm mutations. The C-terminal deletions were generated by use of the Erase-a-Base kit from Promega as described previously (*33*). The generation of His-S-SStp, an epitope-tagged form of the full-length transit peptide for preSSU, was described in ref *34*.

Overexpression of Toc34DTM, PreOE33, PreOE23, PreSSU, and the Mutants of PreSSU. The creation of the overexpression vector as well as detailed protocol for expression of Toc34ΔTM-6×His is described elsewhere (*7*). PreSSU was overexpressed and purified as described previously (*35*). The mutants of preSSU, preOE33, preOE23, and His-S-SStp were expressed as described (*36*, *34*). Inclusion bodies were solubilized in 25 mM Hepes, pH 7.6, 8 M urea, and 50 mM DTT.

Structure Prediction. psToc34 (*Pisum sativum*), atToc33 and atToc34 (*A. thaliana*), and zmToc34-1 and zmToc34-2 (*Zea mays*) were aligned by use of ClustalW 1.8 and MAP (searchlauncher.bcm.tmc.edu/multi-align/multi-align.html). The secondary structure of all five proteins was predicted from the following programs: an alignment-based prediction program (PSI-pred, *37*), an amino acid pair prediction program (GOR4, *38*), a protein class prediction program (DPM, *39*), the neuronal network-based prediction program (PHD, *40*), a program based on the conformational propensities of the residues (DSC, *41*), a program combining the nearest-neighbor information about residues and multiple sequence alignments (NNSSP, *42*), and a program that uses pairwise local alignments and an algorithm for identification of hydrogen-bonded pairs (Predator, *43*). All programs are freeware on the Internet. Then the secondary structure predictions for each protein were aligned in order to increase the reliability of the prediction for each protein. The final secondary structure prediction of all five proteins was aligned according to the results from ClustalW 1.8 and MAP.

Circular Dichroism, Fluorescence, and Absorption Spectroscopy Measurements. Circular dichroism spectra were recorded in 10 mM Hepes/KOH, pH 7.6, and 100 mM NaCl on a Jobin Yvon CD6 spectrometer (Division d'Instruments SA) in a cuvette with 1 mm path length for far-UV and 10 mm path length for near-UV recording at 22 °C with 1 nm steps, 1 s integration time, and a slit width of 2 nm. Depending on the signal/noise of the spectrum, up to 15

spectra were recorded and averaged. The further manipulations of the rough data are described in refs *24* and *44*. For determination of unfolding parameters, Toc34ΔTM was incubated for 24 h at 4 °C with the denaturant at the indicated concentration. The sample was then equilibrated at 22 °C for 30 min and spectra were recorded. The conditions of CD spectroscopy are described above. Absorption spectra were recorded between 300 and 260 nm on a Shimadzu UV-1602 spectrophotometer (Shimadzu, Europe GmbH) in a 10 mm cuvette at a scan rate of 1 nm/s and a slit width of 2 nm. The fluorescence spectrum for tyrosine was recorded on a Hitachi F4500 fluorescence spectrometer (Hitachi, Japan). The excitation wavelength was set to 274 nm with a 2 nm slit width and the emission was recorded for 1 min at 303 nm with a slit width of 4 nm. As a control, an emission spectrum was recorded between 290 and 320 nm. After recording, the samples containing 4 M GuHCl or 6 M urea were diluted 10-fold into 10 mM Hepes/KOH, pH 7.6, and 100 mM NaCl, and CD and fluorescence spectra was recorded to confirm reversibility of folding. Folding parameters were calculated as described (*44*).

Competition of PreSSU Import by the Cytosolic Domain Toc34. Chloroplasts were isolated as described (*8*). PreSSU was radiolabeled with [^{35}S]methionine by in vitro translation with either the wheat germ or the rabbit reticulocyte lysate systems (*45*). The individual components (nucleotides, preSSU, Toc34, and chloroplasts) were combined and allowed to incubate for 10 min. The final import reaction was conducted at room temperature for 5 min and initiated by the addition of 5 mM MgATP (*46*). Chloroplasts were reisolated and subjected to SDS−PAGE analysis and fluorography. The radioactivity associated with preSSU and mSSU was quantified by scintillation counting after the dried SDS−PAGE gel slices were dissolved in 30% H_2O_2 and 60% $HClO_4$ for 16 h at 60 °C. The values were normalized to the value of mSSU imported in the absence of Toc34 or GTP addition to the prebinding step and represent the average of three independent experiments.

Activation of IAsys CMD Cuvette with Ni−NTA. The IAsysPlus double cuvette system (Affinity Sensors, Cambridge, U.K.) was used to determine binding constants. Protein was immobilized by a protocol adopted from the manual. In detail: each chamber of the (carboxylmethyl)-dextran-coated cuvette was incubated with 70 μL of HBST (10 mM Hepes/KOH, pH 7.4, 138 mM NaCl, 2.7 mM KCl, and 0.05% Tween 20) until a stable baseline was observed. Then 100 μL of a fresh mixture containing 100 mM 1-ethyl-3-(3-dimethylaminopropyl)carbodiimide and 29 mM *N*-hydroxysuccinimide (EDC/NHS) was added. After 15 min EDC/NHS was added a second time for 15 min. When the cuvette was reactivated, this step was repeated once more; otherwise both chambers were washed 3 times with HBST and left in HBST for 1 min. The buffer was then replaced by 33 μL of 100 mM NTA (Qiagen, Hilden, Germany) and cuvettes were incubated for 10 min. Both chambers were washed three times with HBST and then incubated for at least 1 min in the same buffer. Additional coupling sites were blocked for 2 min by addition of 100 μL of 1 M ethanolamine, pH 8.5. Nickel was loaded by incubation with 50 mM nickel sulfate in 10 mM Hepes/KOH, pH 8.0, for 5min. This step was repeated three times, followed by three wash steps with HBST. Both chambers were washed twice with 90 μL of PGIW buffer (50 mM sodium phosphate, pH 6.8, 10% glycerol, 300 mM imidazole, and 300 mM NaCl) followed by a 3 min incubation in the same buffer. The buffer was replaced by three washes with HBST and both chambers were maintained under the same buffer until use. The cuvettes were stored between experiments at 4 °C under HBST with 0.02% sodium azide.

Immobilization of His-Tagged Proteins to IAsys Ni−NTA Cuvette. Prior to use, His-tagged proteins were dialyzed for 16 h against 10 mM sodium phosphate, pH 8, 50 mM NaCl, 5% glycerol, 0.7 mM β-mercaptoethanol, and 0.01% Triton. Proteins were diluted at least 10 times to a final concentration of 0.1 μg/μL with HBST, and 100 μL was incubated in each chamber until equilibrium was reached. Both chambers were washed with HBST and incubated until equilibrium was reached again. This procedure was repeated 3−5 times to yield between 0.5 and 15 nM (in 100 μL reaction volume) coupled protein on the IAsys cuvette surface using the published signal:protein ratio of 50 arcsec/ng of immobilized protein (manual). Finally both chambers were incubated with HBST until experiments were performed.

Binding Experiments with the IAsys Cuvette. Both chambers of the Ni−NTA cuvette were filled with 90 μL of the binding buffer (20 mM Hepes/KOH, pH 8.0, 50mM NaCl, 0.05% Triton X-100, 2.5% glycerol, and 0.01% fatty acid-free BSA) and allowed to equilibrate. A new baseline was established for ∼2 min and binding was initiated by injection of 1−10 μL of the indicated amounts of proteins into their respective chambers as described in the figure legends. When binding was performed in the presence of GTP, 0.5 mM $MgCl_2$ was added. Dissociation was performed in 90 μL of the same buffer (except GTP). For surface regeneration between experiments, both chambers were extensively washed with 20 mM Hepes/KOH, pH 8.0, 150 mM NaCl, 0.1% Triton X-100, 2.5% glycerol, and 0.01% BSA.

After a completed set of experiments, the bound His-tagged protein was stripped with 20 mM Hepes/KOH, pH 7.0, 500 mM imidazole, and 0.1% Triton X-100, and nickel was removed by addition of 50 mM EDTA, pH 8.0. After several washes the cuvette was stored at 4 °C in HBST. The cuvette was recharged with Ni^{2+} prior to protein loading in subsequent experiments.

In some cases (Toc34ΔTM and for some experiments preSSU and preOE33) His-tagged proteins were used as ligand. The use of His-tagged ligands was possible for two reasons. First, the association of preSSU containing and not containing a His tag with immobilized Toc34 was found to be identical (not shown). Second, for all measurements where a His-tagged ligand was used, self-immobilization could not be observed as controlled in the parallel cuvette (not shown).

Analysis and Quantification of IAsys Biosensor Binding Curves. Data files from IAsys plus were further analyzed with SigmaPlot 5.0. (SPSS Inc.). Association curves were analyzed by nonlinear regression of the data to

$$R = R_{eq}[1 - \exp(-k_{on}t)] + R_0 \qquad (1)$$

where t is the time in seconds, R is the response in arcsecs, R_0 is the initial response (baseline), R_{eq} is the response at equilibrium, and k_{on} is the first-order rate constant of interaction in reciprocal seconds. After analysis of the association curves, the dissociation constant K_D can be

derived by a nonlinear regression of the plot between the R_{eq} values and the ligand concentration [L]:

$$R_{eq} = R_{max}[L]/(K_D + [L]) \quad (2)$$

where R_{max} is the maximal possible response. The calculated maximal response was compared with the expected maximal response ($R_{max,exp}$):

$$R_{max,exp} = R_{im}MW_L/MW_{im} \quad (3)$$

with R_{im} being the response during immobilization, MW_L the molecular weight of the ligand, and MW_{im} the molecular weight of the immobilized protein. Dissociation curves were analyzed by nonlinear regression of the data to

$$R = (R_{eq*}) \exp(-k_{diss}t) + R_0 \quad (4)$$

where R_{eq*} is the initial response when dissociation is started and k_{diss} is the dissociation rate constant in reciprocal seconds. The dissociation constant K_D is defined as

$$K_D = k_{diss}/k_{ass} \quad (5)$$

The association constant k_{ass} can be extrapolated by linear regression of a plot of the first-order rate constant k_{on} and the ligand concentration [L]:

$$k_{on} = k_{ass}[L] + k_{diss} \quad (6)$$

From eqs 2, 5, and 6, two extrapolations can be made. When a response at the equilibrium R_{eq} significantly lower than the maximal expected response $R_{max,exp}$ is observed, eq 2 can be rewritten as

$$K_D = (R_{max,exp} - R_{eq})[L]/R_{eq} \quad (7)$$

In the case that a ligand concentration significantly higher than the concentration of the immobilized protein is used in such a way that association is not limited by the concentration of the ligand, the K_D can be calculated from a combination of eqs 5 and 6:

$$K_D = k_{diss}[L]/(k_{on} - k_{diss}) \quad (8)$$

However, eqs 7 and 8 give only an approximate value for the dissociation constant.

RESULTS

Structural Features of Toc34. To analyze the association of Toc34 and chloroplast transit peptides, we expressed a recombinant, highly soluble Toc34 in *Escherichia coli* that lacks the C-terminal residues 252−310 including the transmembrane domain (Toc34ΔTM). The truncated Toc34 was purified by use of its C-terminal His tag (Figure 1A, compare lanes 1 and 2) to near homogeneity (Figure 1A, lane 3). This polypeptide was used to investigate the structural features of the soluble, cytosolic domain of Toc34 by CD spectroscopy (Figure 1B). The cytosolic domain contains 34% helical structure, 26% β-sheets/β-turns, and 40% random coil structure as determined by deconvolution of the far-UV−CD spectrum. The analysis of the amino acid sequence by secondary structure prediction algorithms (described under Materials and Methods) revealed 36% helical structure and

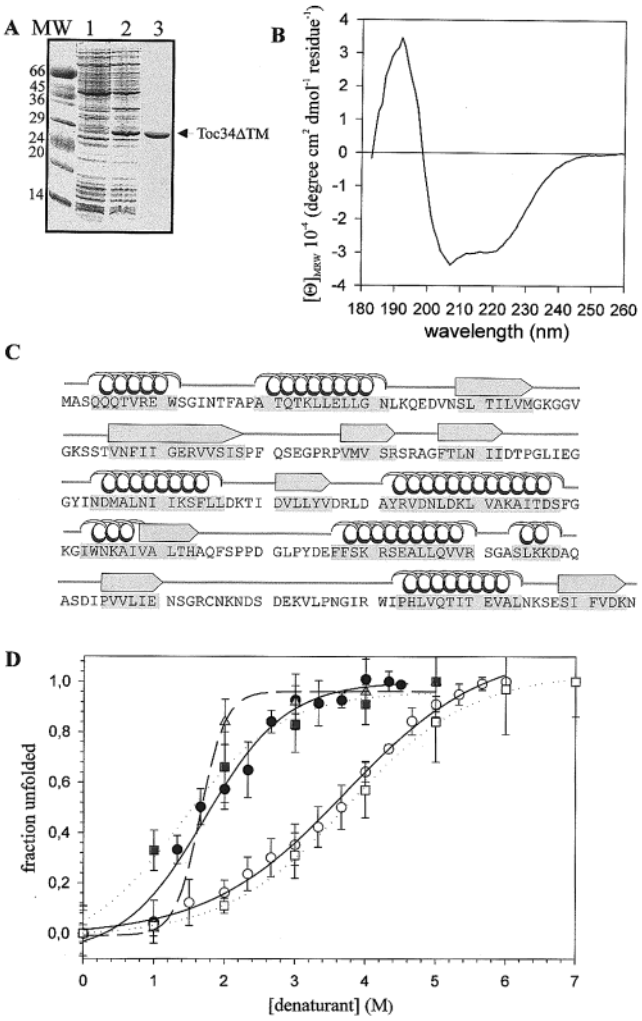

FIGURE 1: Overexpressed Toc34 contains secondary structure elements. (A) Toc34ΔTM-6×His was expressed in *E. coli*. Lane 1 shows noninduced cells; lane 2, the same cells 3 h after induction; lane 3, the purified protein. (B) Shown is the far-UV CD spectrum of Toc34ΔTM (30 μM) recorded as described. This spectrum was used to calculate the secondary structure content. (C) Structure prediction of Toc34 performed as described under Materials and Methods. (D) Toc34ΔTM was incubated for 24 h with the indicated amount of denaturant (GuHCl, solid symbols, or urea, open symbols), and unfolding was determined at 222 nm by CD-spectroscopy (circles, solid line), by tyrosine fluorescence at 303 nm (triangles, dashed line), and by tryptophan absorption at 280 nm (squares, dotted line). The calculated values from these curves are given in Table 1.

20% β structure (Figure 1C), which is in good agreement with the values obtained from CD spectroscopy. The near-UV CD spectrum of Toc34ΔTM (not shown) is less informative, since Toc34 contains multiple aromatic residues (9 Phe, 4 Tyr, and 3 Trp) contributing to the signal.

Using CD spectroscopy, tyrosine fluorescence, and tryptophan absorption, we also explored the stability of folding of the truncated Toc34ΔTM by chemical denaturation. Denaturation with GuHCl revealed smaller $D_{1/2}$ and $\Delta G_{d,aq}$ values than denaturation with urea (Figure 1D and Table 1) (*44*, *47*). The $D_{1/2}$ value reflects the concentration at which half of the molecules are in an unfolded state, and $\Delta G_{d,aq}$ represents the minimal value of the conformational stability of the protein in the absence of the denaturant. The results suggest that the tertiary structure of Toc34ΔTM is stabilized by electrostatic interaction.

Table 1: Unfolding Parameters of the Cytosolic Domain of Toc34

denaturant	method	m^a (kcal mol^{-1} M^{-1})	$D_{1/2}{}^b$ (M)	$\Delta G_{d,aq}{}^a$ (kcal/mol)
urea	CD[c]	0.6	3.7	2.2
urea	Trp[d]	0.7	3.8	2.6
GuHCl[e]	CD	1.0	1.8	1.8
GuHCl	Trp	0.8	1.5	1.2
GuHCl	Tyr[f]	3.4	1.7	5.6

[a] Calculated by eq 4 in ref *44*. [b] Calculated by itting the data to a sigmoidal equation by least-squares analysis. [c] Circular dichroic spectroscopy. [d] Tryptophan absorption [e] Guanidine hydrochloride. [f] Tyrosine fluorescence.

To probe the environment of the aromatic amino acids, the denaturation of Toc34ΔTM was followed by Tyr fluorescence and Trp absorption (Figure 1D and Table 1). Analysis of the unfolding by Trp absorption (A_{280}) revealed similar results as observed for the secondary structure by CD spectroscopy, suggesting that several of the Trp are at least partially exposed to the solvent. When Tyr fluorescence was used to monitor the GuHCl-induced unfolding of Toc34ΔTM, a $D_{1/2}$ value similar to that observed by the other detection methods was determined (Figure 1D and Table 1). However, higher m and $\Delta G_{d,aq}$ values were observed. It has been proposed that an increase in the m value represents an increase of the surface area of the protein upon exposure to the denaturant (*48*). Therefore, the result suggests that, in contrast to the surface-exposed Trp residues, the four Tyr are buried more deeply into the core of Toc34ΔTM.

Comparison of the proposed secondary structure of the GTPase domain of Toc34 (*8*, *49*) to the secondary structure of hRas21p and Rap2p, two GTPases with highest homology to Toc34, revealed a similar secondary structure. hRas21p has a helical content of 34% and a β structure content of 27% (*50*), and Rap2p has a helical content of 38% and a β structure content of 27% (*51*). The similarity of the secondary structure of related GTPases and Toc34ΔTM as well as the features of Toc34ΔTM during chemical denaturing suggest that the heterologously expressed Toc34ΔTM folds into a secondary structure similar to that of other well-characterized GTPases.

Addition of the Cytosolic Domain of Toc34 Inhibits in Vitro Import of PreSSU. To determine if the soluble, cytosolic domain of Toc34 is able to interact with a transit peptide of a preprotein, an in vitro import inhibition assay was developed. Since Toc34ΔTM could also indirectly inhibit preprotein binding/import by remodeling or altering the organization of the outer envelope translocon, different order-of-addition schemes were invoked (Figure 2). Previous results indicate that Toc34 recognizes a phosphorylated form of preSSU with higher affinity (*7*). Therefore, both the phosphorylated and nonphosphorylated forms of preSSU were tested. Transit peptide phosphorylation of the preprotein was achieved by in vitro translation of preSSU in a wheat germ lysate (*45*). The results were quantified and compared to the translocation efficiency of preSSU without any additions (standard import).

Addition of GTP to the chloroplasts prior to the import reaction did not result in a significant change of the import efficiency of the phosphorylated preprotein (Figure 2, upper gel, lane 2) in comparison to standard import conditions (upper gel, lane 1). The import of the nonphosphorylated

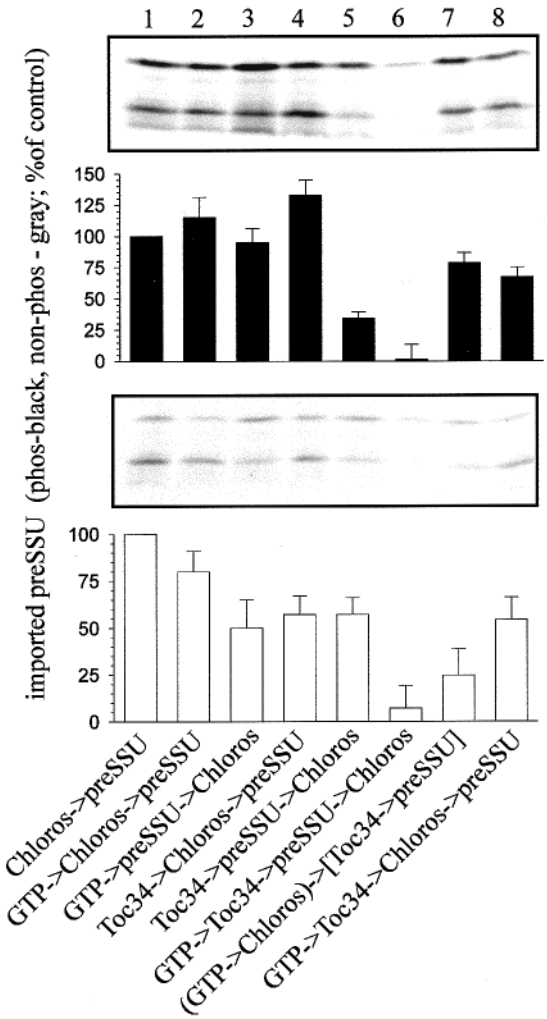

FIGURE 2: Toc34ΔTM inhibits import of phosphorylated and nonphosphorylated preSSU. The import of [^{35}S]methionine-labeled in vitro-translated preSSU by the wheat germ system (phosphorylated preSSU, upper gel and histogram) or the rabbit reticulocyte lysate (nonphosphorylated preSSU, lower gel and histogram) into chloroplasts (10 μg of chlorophyll) was performed in the presence of 1 mM GTP (lanes 2, 3, and 6−8) and 4 μM Toc34ΔTM (lanes 4−8). Shown is the quantification of inserted preSSU (maturated) of at least four independent experiments; error bars indicate the standard deviation. The sequence of pipetting is indicated.

preprotein was slightly reduced (lower gel, lane 2). When GTP was added to preSSU prior to the addition of chloroplasts (lane 3), we observed no influence on the import of the phosphorylated preprotein but a reduction of import of the nonphosphorylated preprotein by 50%.

When Toc34ΔTM was added to chloroplasts prior to the addition of the preprotein, the import of the phosphorylated preprotein was stimulated while the translocation of the nonphosphorylated preprotein was reduced (Figure 2, lane 4 vs lane 1). However, a drastic reduction of import of the initially phosphorylated preprotein was observed when Toc34ΔTM was added to the preprotein prior to the addition of chloroplasts (upper gel, lane 5 vs lane 1). Addition of the nonphosphorylated preprotein to Toc34ΔTM reduces the import as much as addition of Toc34ΔTM to the chloroplasts directly (lower gel, lane 5 vs lane 4) but not as drastically as for the phosphorylated preprotein form (upper gel, lane 5). This is consistent with the observation that Toc34 has a lower affinity for the nonphosphorylated preprotein, and

therefore more preprotein remains import-competent in the import mixture.

Toc34 has a higher affinity for transit peptides when it is in the GTP-bound form (*7*). Therefore, we investigated the import inhibition using Toc34ΔTM in the presence of GTP (Figure 2, lanes 6−8). First, the Toc34ΔTM was incubated with GTP prior to the addition of preSSU. Import into chloroplasts was completely inhibited for the phosphorylated and the nonphosphorylated preprotein (lane 6 vs lane 1). When GTP was initially added to the chloroplasts and Toc34ΔTM was preincubated separately with preSSU (lane 7), the translocation of the preprotein was reduced but not abolished as above. The translocation efficiency of the initially phosphorylated preprotein was significantly higher when the latter pipetting sequence was used than in the absence of GTP (upper gel, lane 7 vs lane 5). This might be explained by preloading of endogenous Toc34 and Toc159 with GTP, resulting in a higher affinity for preSSU than Toc34ΔTM (upper gel, lane 2). Import is decreased by 50% when Toc34ΔTM and GTP are added to the chloroplasts prior to phosphorylated preSSU (upper gel, lane 8) but still not as drastic as in lane 6. Under similar conditions the insertion of the nonphosphorylated preprotein was also reduced to 50% (lower gel, lane 8). These observations underline the GTP influence of receptor−preprotein interaction.

Nucleotides Modulate the Affinity of Toc34ΔTM for Preproteins. The data (Figure 2) indicate that Toc34 interacts directly with preproteins. To investigate the kinetics of this interaction in detail, we utilized an IAsys Biosensor. This biosensor uses a dual-chamber cuvette and a resonance mirror technique to monitor macromolecular interactions (*52*). His-tagged Toc34ΔTM was immobilized to a NTA−Ni^{2+}-modified carboxymethylated dextran-coated cuvette as described under Materials and Methods. Typically, one chamber was loaded with Toc34ΔTM whereas the other chamber was used for baseline control (Figure 3A). After coupling, the signal for both cuvettes was set to zero (Figure 3A, equilibration) and the different preproteins or transit peptides were added to both cuvettes (Figure 3A, association). Often, a background signal was observed (Figure 3A) due to a buffer shift or slow precipitation of the ligands. The kinetic of ligand binding is indicated by an increase in the response in arcsecs, which reflects an increase in the mass of protein near the surface of the cuvette. The dissociation of the ligands was initiated by changing the buffer (Figure 3, dissociation) and the dissociation was detected. After recording the dissociation, the cuvette was washed several times (Figure 3A, wash) and reequilibrated to be used for the next binding experiment (Figure 3A, equilibration). If an equilibrium could not be reached, Toc34ΔTM was stripped from the cuvette and the chamber was reloaded with fresh receptor. The association of ligands was then analyzed after baseline correction by nonlinear least-squares fit to eq 1 as demonstrated in Figure 3B.

After immobilization of Toc34ΔTM to the surface of the cuvette, preSSU, preOE23, or preOE33 was added in the presence of GTP (Figure 4A). As shown in Figure 4A, all preproteins interact with the receptor Toc34 in the presence of GTP. However, the association efficiency seems to differ. To outline the influence of GTP and GDP on the interaction between Toc34ΔTM and preproteins, the binding between

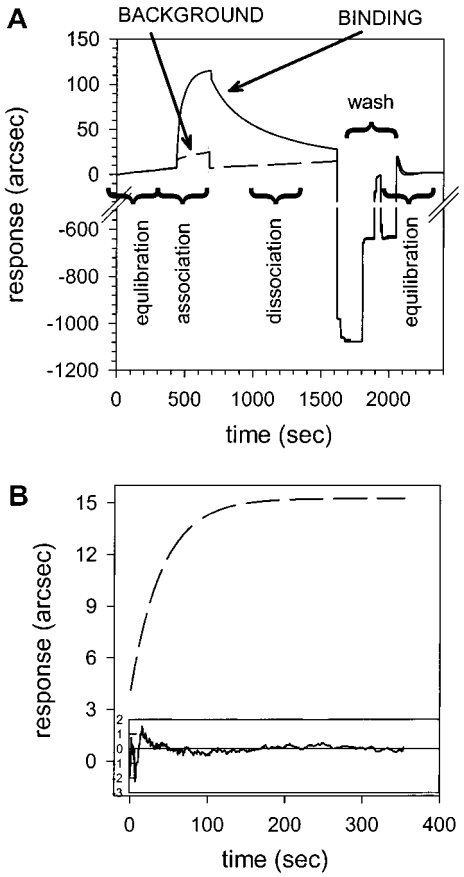

FIGURE 3: Recording and analysis of the association of proteins with the IAsys Biosensor. (A) Toc34ΔTM was immobilized as described under Materials and Methods to a final concentration of 6.0 nM into chamber 1 (binding), whereas chamber 2 was left without coupling (background). After coupling, the signal was set to zero (equilibration). Then 102 nM preSSU was added in the absence of nucleotides and the association curve was recorded (association). Buffer was changed to monitor dissociation. To reuse the cuvette, both chambers were washed several times (wash) and reequilibrated for the next experiment (equilibration). (B) 6.8 nM His-S-SStp was immobilized and association of 72 nM Toc34ΔTM in the presence of 1 mM GTP was recorded as described for panel A. Shown is the association curve corrected for background (solid line), the least-squares analysis to eq 1 (dashed line) and the residuals to the fit (inset below).

Toc34ΔTM and preSSU or preOE33 was studied in more detail.

Identical amounts of preSSU were added to Toc34ΔTM in the presence of GTP or GDP or in the absence of nucleotides (Figure 4B). The observed association was strongest in the presence of GTP and was drastically reduced in the presence of GDP or in the absence of nucleotides (Figure 4B). This is also reflected by the maximal association R_{eq} (not shown) or the dissociation constant K_D (Table 2). Further, the addition of ATP did not enhance the association of the nonphosphorylated preSSU (Table 2), being in line with the effect of ATP on the interaction of phosphorylated preSSU with Toc34 (*7*). In addition, the first-order on-rate constant in the presence of GDP but not in the absence of nucleotides is 2-fold lower, suggesting a slower association (Table 2). The dissociation rate constants of the complex between preSSU and Toc34 is 3 times higher when GTP was not present (Table 2).

The nucleotide dependence of the interaction of preOE33 with Toc34ΔTM was different from the interaction of

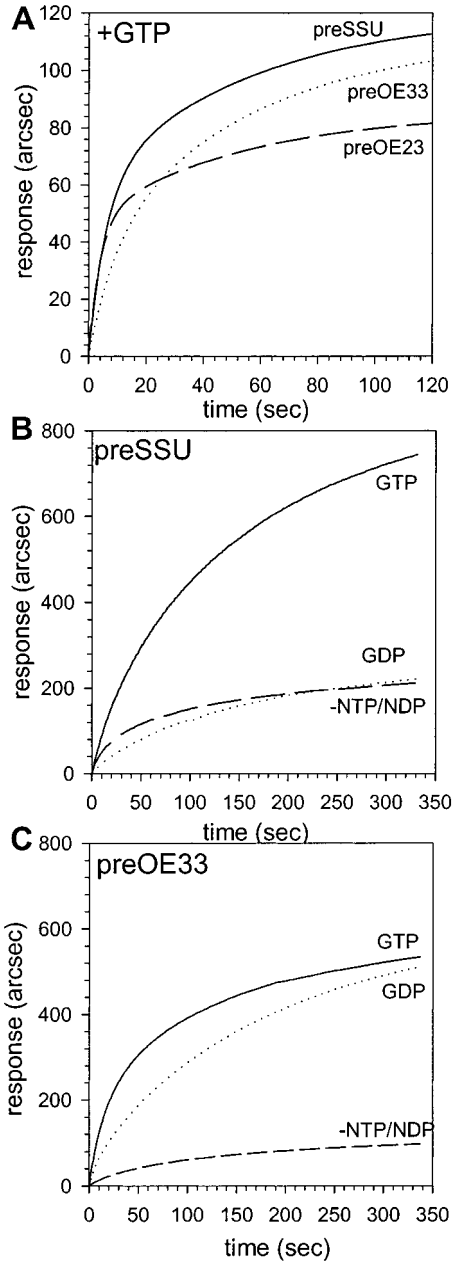

FIGURE 4: Interaction of preSSU, preOE23, and preOE33 with Toc34 is GTP-dependent. Toc34ΔTM was immobilized to a final concentration of 0.64 nM (A) or 6.0 nM (B, C). In panel A, 370 nM preSSU, 1140 nM preOE33, or 1100 nM preOE23 was added in the presence of 1 mM GTP. PreSSU (205 nM, panel B) and preOE33 (311 nM, panel C) were bound to Toc34ΔTM in the presence of 5 mM GTP (solid lines) or 5 mM GDP (dotted lines) or in the absence of nucleotides (dashed lines).

preSSU with Toc34ΔTM (Figure 4C). The first-order on-rate constant of the association of preOE33 in the presence of GTP is comparable to the first-order on-rate of preSSU (Table 2). In contrast to the observation of the dissociation of preSSU, the dissociation rate constant for preOE33 in the presence of either GDP or GTP was comparable (Table 2). Only in the absence of nucleotides was the dissociation rate constant for preOE33 changed: it was about 5-fold higher (Table 2). The same was observed for the responses at equilibrium (Figure 4C). The dissociation constants (Table 2) of the Toc34ΔTM−preOE33 complex in the presence of GTP is only 3−4-fold lower than in the presence of GDP, which is in contrast to the observation made for the

Table 2: Association and Dissociation Rate and Dissociation Constants of Toc34, preSSU, and Peptides

protein	nucleotide	k_{on} (s^{-1})	k_{ass}[a] (M^{-1} s^{-1})	k_{diss}[b] (s^{-1})	K_D[c] (nM)
preSSU	GTP	0.017[d]	9.1×10^5	0.010	24 ± 6
preSSU	GDP	0.008[d]	nd[e]	0.030	310[f]
preSSU	ATP	0.014	nd	0.031	190[f]
preSSU		0.015[d]	3.1×10^5	0.029	140 ± 30
preOE33	GTP	0.018[d]	nd	0.012	23[f]
preOE33	GDP	0.008[d]	nd	0.016	86[f]
preOE33		0.009[d]	nd	0.053	572[f]
B1	GDP	0.027[g]	nd	0.023	$90\,000 \pm 10\,000$
B1	GTP	0.030[g]	1.1×10^3	0.017	$25\,000 \pm 5000$
A1	GTP	0.028[g]	nd	0.033	$210\,000 \pm 20\,000$
E2	GTP	0.016[g]	nd	nd	400 000[h]

[a] Calculated by eq 6. [b] Calculated by eq 4 and averaged for different experiments. [c] Calculated by eqs 2 and 5. [d] Values taken from Figure 4. [e] Not determined. [f] Calculated by eq 8. [g] Taken from Figure 6. [h] Calculated by eq 7.

interaction of preSSU with Toc34ΔTM. Only the dissociation constant in the absence of nucleotides is drastically increased (Table 2). This is due to the lower on rate and the increased dissociation rate of preOE33 from Toc34ΔTM. Therefore, even though Toc34ΔTM recognizes both preproteins with highest affinity in the presence of GTP, the nucleotide dependence of the interaction is altered.

To determine the dissociation constant of the interaction of Toc34ΔTM and preSSU more precisely, different amounts of preSSU were added to the immobilized Toc34ΔTM in either the presence or absence of GTP. By use of eq 1, the response in arcsecs at equilibrium was calculated from the association curves and plotted against the ligand concentration (Figure 5A). To calculate the association rate constant, the first-order rate constants were plotted against the ligand concentration (Figure 5B). The association rate was found to be on the order of 10^6 M^{-1} s^{-1} for the binding in the presence of GTP and 3×10^5 M^{-1} s^{-1} in the absence of nucleotides, which resembles the trend observed for the first-order rate constants. The averages of the dissociation constants derived by the classical calculation (eq 5) and from Figure 5A (eq 2) are given in Table 2.

Interaction of Toc34 Is Mediated by the Transit Peptide. To address whether the mature domain of preSSU itself is able to associate with the truncated form of Toc34, we tested a purified form of mSSU. As shown in Figure 5C, preSSU rapidly interacts with Toc34 reaching a plateau in less than a minute. The addition of a similar amount of mSSU fails to generate a response higher than background (Figure 5C) even if it is allowed to bind for 10 min (data not shown). We conclude that the mature domain of SSU itself does not interact with Toc34. Moreover, this experiment demonstrates that the use of chemically denatured proteins does not lead to any significant nonspecific absorption of a protein to Toc34 upon rapid dilution.

To determine a possible influence of the mature domain on the interaction of the presequence with Toc34ΔTM, we used three previously described preSSU mutants (*33*). In those mutants 52, 67, or 75 C-terminal located amino acids of the mature domain were deleted. As in Figure 5A, several concentrations of the mutants were incubated with Toc34 in the presence of GTP. The resulting equilibrium values of the response were plotted against the concentration of

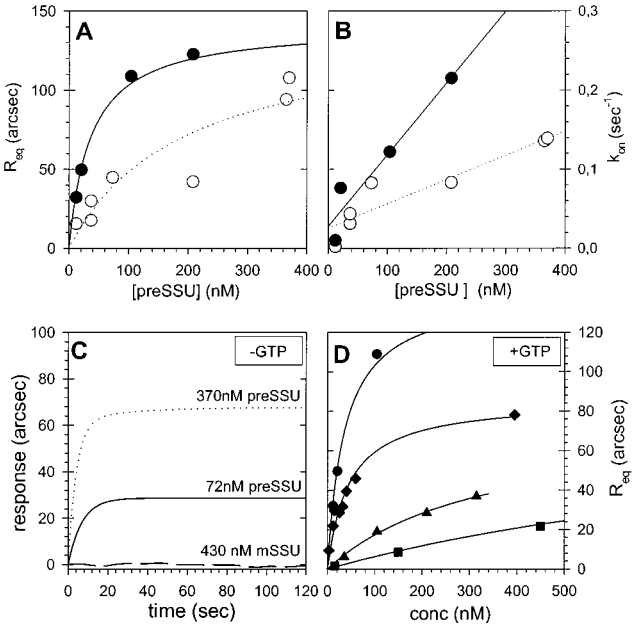

FIGURE 5: Interaction between Toc34 and preSSU is dependent on the transit sequence but influenced by the C-terminus of the mature domain. The interaction of different concentrations of mSSU, preSSU, and C-terminal deletion mutants and immobilized Toc34 (6 nM in panels A and B; 0.64 nM in panel C; 1.16 nM in panel D) were performed as in Figure 4. (A) Equilibrium values of the resonance of the interaction of preSSU and Toc34 in the presence of 1 mM GTP (●) or 1 mM GDP (○) were plotted against the concentration of preSSU used. Lines represent the least-squares analysis with a hyperbolic function according to eq 2. (B) First-order on-rate constants of the interaction between Toc34 and preSSU in the presence of 1 mM GTP (●) or 1 mM GDP (○) were plotted against ligand concentration. Lines represent results of linear regression according to eq 6. (C) PreSSU (370 nM, dotted line, or 72 nM, solid line) and mSSU (430 nM, dashed line) were incubated with Toc34 in the absence of GTP. (D) Interaction between immobilized Toc34 and preSSU (●), preSSUD52 (◆), preSSUD67 (▲), and preSSUD72 (■) was determined and the equilibrium values were plotted against ligand concentration. The lines represent the least-squares analysis with a hyperbolic function according to eq 2.

Table 3: Dissociation Constants and Change of the Gibbs Energy during Binding of Length Deletions of Nonphosphorylated PreSSU to Toc34ΔTM in the Presence of GTP

protein	K_D (nM)	$\Delta G_{binding}$[d] (kJ/mol)
preSSU	24[a]	−42.7
preSSUΔ52	45[b]	−41.2
preSSUΔ67	340[b]	−36.3
preSSUΔ75	1 300[b]	−33.0
preSSU − tp	6 300[c]	−29.1
tp C-term (A1)	210 000[a]	−20.6
tp N-term (E2)	400 000[a]	−19.1

[a] Values taken from Table 2. [b] Calculated from values in Figure 5D by eq 2. [c] Calculated by eq 7. [d] The Gibbs energy change of the interaction was calculated by $\Delta G_{binding} = -RT \ln (1/K_D)$.

preSSU or its mutants (Figure 5D). The association of the preprotein lacking the last 52 amino acids of the mature domain with Toc34ΔTM in the presence of GTP was already decreased by a factor of 2 (in Figure 5D; Table 3). Deletion of the C-terminal 67 amino acids resulted in a more drastic reduction of the affinity. In the presence of GTP the observed dissociation constant was 10-fold higher than the dissociation constant of the wild-type preSSU. Deletion of 75 amino acids from the C-terminus of preSSU increased the dissociation constant even more, by a factor of 50 (Table 3).

To confirm that the transit peptide alone is capable of interacting with Toc34, we immobilized His-S-SStp, an epitope-tagged form of the full-length transit peptide for preSSU (*34*), to the cuvette and tested for Toc34 binding in the presence of GTP (Figure 3B). Remarkably, Toc34 still recognizes the transit peptide, even though its N-terminus is immobilized, suggesting that the interaction between the receptor and the transit peptide requires a region of the protein distal from the N-terminus. The dissociation constant for this interaction is 230-fold higher compared to the dissociation constant found for full-length preSSU (Table 3). We conclude that the association of Toc34 with preSSU is positively modulated by the mature domain via an unknown mechanism but does not involve a direct association between Toc34 and mSSU (Figure 5C). However, the association is initiated by the transit peptide.

Interaction of Toc34 with Peptides of the Transit Sequence of PreSSU. To identify the region of the transit peptide of preSSU that is recognized by Toc34ΔTM, we utilized synthetic peptides that correspond to the N-terminal half (E2) and the C-terminal half (A1) of the transit peptide (Figure 6A). The transit peptide can be phosphorylated at serine at position 34 (*35*), which is present in A1. The phosphorylated form of A1, denoted B1, was then used to investigate the influence of transit peptide phosphorylation on the interaction with the Toc34 receptor. We observed that all three peptides are able to bind the immobilized Toc34 when added in the presence of GTP (Figure 6B). The phosphorylated peptide, B1, showed the highest binding affinity. The peptide representing the N-terminal domain, E2, displayed the lowest association even though it was present at a 5-fold higher concentration (Table 2). In the presence of GDP, the association of the phosphorylated peptide but not of the nonphosphorylated peptide was decreased (Figure 6C). The association of the N-terminal region of preSSU (E2) was decreased almost to baseline level when GDP or no nucleotide was present (Figure 6C,D). When A1 and B1 were added in the absence of nucleotides, A1 binding was decreased to background level, whereas an interaction between B1 and Toc34 was still detectable (Figure 6D). Interestingly, first-order rate constants did not depend on nucleotides (Table 2). The dissociation constant calculated from eq 7 was low for the N-terminal region for Toc34 even in the presence of GTP (Table 2). The affinity of the nonphosphorylated peptide A1 is similar in the presence of GTP and GDP but decreased in the absence of nucleotides. The highest affinity was found for the phosphorylated peptide (see below).

To investigate the influence of the transit peptide phosphorylation in more detail, the association of A1 and B1 with Toc34 was determined at different ligand concentrations in the presence of both GTP and GDP. Figure 6E shows the relationship between the response at the equilibrium in arcsecs and the ligand concentration. From this analysis the measured dissociation constants shown in Table 2 demonstrate that Toc34 has a significantly higher affinity for the phosphorylated peptide than for the nonphosphorylated peptide. Further, this interaction is increased when GTP is present. The differences observed between the K_D values shown in Table 2 is primarily the result of very different

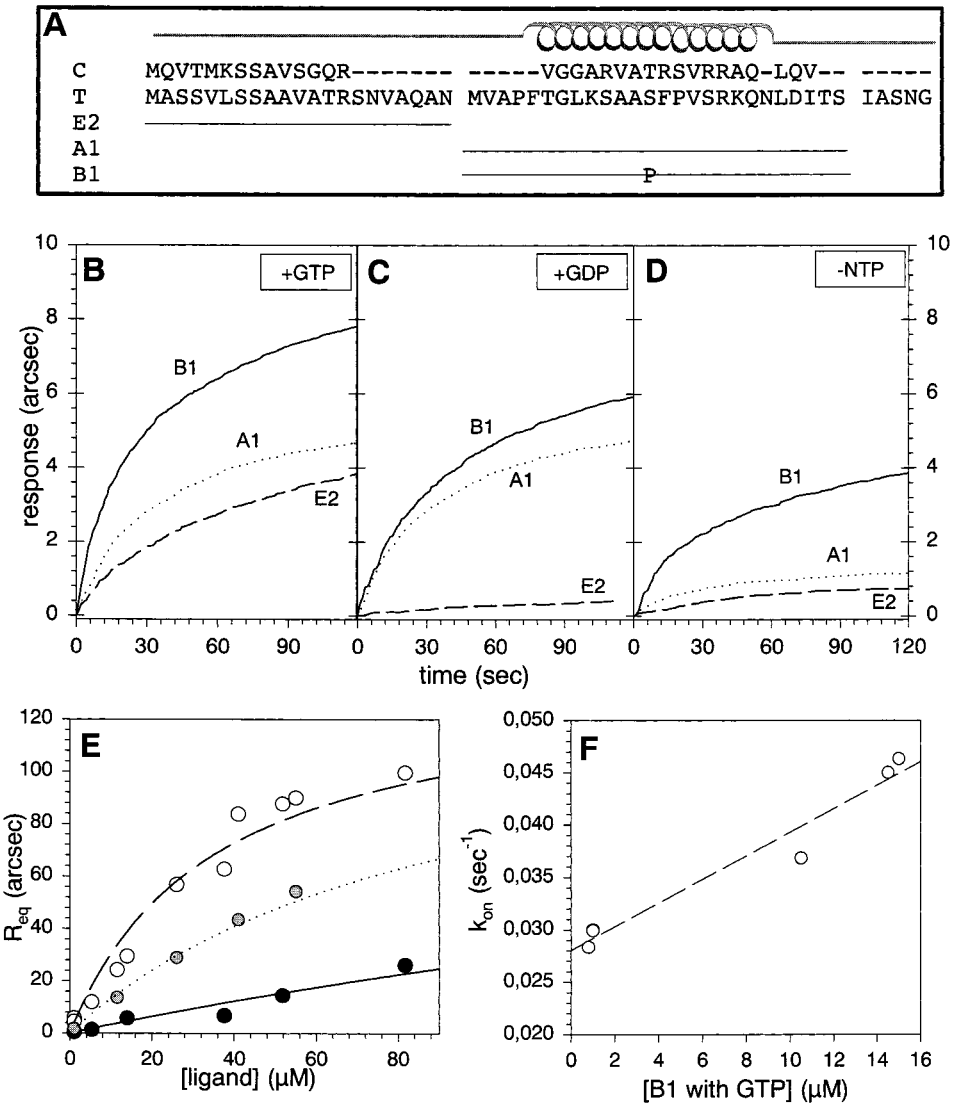

FIGURE 6: Interaction of preSSU with Toc34 is facilitated by the C-terminal portion of the transit peptide and enhanced by transit peptide phosphorylation. (Panel A) Alignment of the transit peptide of the Rubisco activase from *Chlamydomonas* (C) and of the small subunit of Rubisco from tobacco (T) is shown. The secondary structure of the presequence of *Chlamydomonas* is indicated (*27*). The regions of the small subunit of Rubisco from tobacco covered by the peptides are given. The phosphorylation side of peptide B1 is indicted (P). (Panels B−F) Toc34ΔTM (11 nM) was immobilized. In panels B−D the binding of 2 μM B1 (solid line) and A1 (dotted line) as well as binding of 10 μM E2 peptide (dashed line) is shown in the presence of 5 mM GTP (B) or GDP (C) or in the absence of nucleotides (D). Panel E shows the values of the response at the equilibrium of B1 binding in the presence of 5 mM GTP (○) or 5mM GDP (gray circles) and of A1 binding in the presence of 5mM GTP (●). The lines (dashed for B1 with GTP; dotted for B1 without GDP; solid for A1 with GTP) represent the least-squares analysis with a hyperbolic function. Panel F shows the on rates of B1 binding in the presence of GTP in relation to the peptide concentration; the dashed line represents the result of linear regression.

dissociation rates. Furthermore, when an association rate constant for the B1 peptide was determined (Figure 6F), it was found to be 1000-fold lower than the association rate for the full-length preprotein (values given in Table 2). This results in a 1000-fold higher dissociation constant than observed for the preSSU−Toc34 interaction (Table 2). This result indicates that although the C-terminal region is the major determinant of the association of Toc34ΔTM, it is still substantially reduced in its affinity for Toc34 compared to both the full-length transit peptide and the full-length preprotein (Table 3).

Point Mutations in the Transit Peptide InfluenceToc34 Binding of PreSSU. Transit peptide flexibility may be an important structural determinant that may facilitate or enable more favorable interactions between Toc34 and preSSU (*14*). To investigate the role of flexibility, several point mutations were introduced into the transit peptide of preSSU that either add or remove residues that impart peptide flexibility (shown in Table 4). To decrease the transit peptide flexibility, prolines at positions 25 and 36 were mutated to alanines individually in preSSU1-1 and preSSU1-4 and together in preSSU2-1, and the two C-terminal glycines (G52 and G53) were replaced by a serine and an alanine in preSSU1-5. To increase the flexibility, residues A9 (preSSU1-6), M22 (preSSU1-7), A49 (preSSU1-9), A12 (preSSU1-10), V17 (preSSU1-11), and V55 (preSSU1-13) were then mutated into proline residues as shown in Table 4. The preproteins, containing these mutations in the transit peptide, were then purified and tested for their ability to interact with the immobilized Toc34 receptor.

The decreased flexibility influenced the interaction only when the mutation was placed in the C-terminal region of

Table 4. First Order Rate Constants, Dissociation Rate Constants and Dissociation Constants of Interaction between 1.16 nM Toc34 and preSSU and Mutants

Parameter / Ligand	[Ligand] (nM)	k_{on} *10^{-2} (sec^{-1})[a]	k_{diss}*10^{-4} (sec^{-1}) [b]	K_D[c] (nM)	mutation
preSSU	104	3,2	n.s.	24[d]	
preSSU1-1	1438	1,6	1,7	12,9	P25A
preSSU1-4	1300	1,5	9,3	84,8	P36A
preSSU1-5	1350	2,1	3,0	15,0	GG52/53SA
preSSU1-6	1375	1,1	0,7	7,9	A9P
preSSU1-7	913	1,0	4,7	44,8	M22P
preSSU1-9	875	0,8	8,8	69,7	A49P
preSSU1-10	814	0,9	1,2	10,5	A12P
preSSU1-11	912	0,7	1,5	19,5	V17P
preSSU1-13	850	1,2	0,6	3,6	V55P
preSSU2-1	627	1,1	18,1	71,7	P25A/P36A

[a] Calculated by eq 1. [b] Calculated by eq 4. [c] Calculated by eq 8. [d] Average value of the dissociation constant is given.

the transit sequence. Whereas the dissociation constant of preSSU1-1 for Toc34 (Figure 7A) was slightly lower than that of wt-preSSU, the dissociation constant of preSSU1-4 (Figure 7A) was found to be 4-fold lower (Figure 7D and Table 4). The double mutation in preSSU2-1 (Figure 7C) showed the same effect as preSSU1-4, suggesting that the decrease of interaction was due to the replacement of proline 36. When mutations were placed close to the putative cleavage site of preSSU (preSSU1-5 and preSSU1-13; see Table 4), association with Toc34 was increased (Figure 7A,C). The dissociation constant for preSSU1-13 was determined to be 1 order of magnitude lower than for wt-preSSU (Figure 7C,D and Table 4). The increase of flexibility resulted in a similar effect to that observed for the decrease (see above). The association of Toc34 with preprotein mutants decreased with distance of the point mutation from the N-terminus (Figure 7B,C). The point mutations at amino acids 9, 12, and 17 increased the affinity (Figure 7D), whereas all mutations close to or at the C-terminal region showed a reduction of the association with a maximal effect for the replacement of alanine 49 (preSSU1-9, Figure 7D). The only difference was observed for the introduction of a proline at position 55. The dissociation constant of this mutant was found to be 1 order of magnitude lower than that found for wt-preSSU, comparable with the effect of the point mutation at the cleavage site.

The dissociation constant of the mutants was strongly dependent on the localization of the point mutation, which is most effective in the C-proximal position of the transit peptide. This again underlines that the association of Toc34 seems to occur predominantly toward the C-terminal region of the preprotein.

DISCUSSION

Toc34 was originally identified as a core component of the outer envelope translocation apparatus with a typical signature of a GTP binding protein (*8*, *49*). Similar to other GTPases, the heterologously expressed soluble cytosolic domain of Toc34 contains 34% helical structure, 26% β-sheet or β-turn, and 40% random coil as determined by circular dichroism (Figure 1). The cytosolic domain is stabilized by intramolecular electrostatic interactions (Figure 1D and Table 1) since unfolding of Toc34ΔTM revealed an almost 2-fold higher resistance to denaturation by urea compared to GuHCl (Table 1). The folding process of lactalbumin (*53*), a model protein of folding investigations, was compared to the folding of Toc34ΔTM. From that we can conclude that Toc34ΔTM unfolds in a two-step process. In the first step the protein partially unfolds but the core, including the tyrosines (see Figure 1C), is still folded. For the unfolding into this intermediate state an energy of $\Delta G_I = 3.9$ kcal/mol is required. The difference of the *m* values (reflecting the fraction of freshly exposed regions) of the tryptophan and the tyrosine signals further suggests that the four tyrosines are located in the interior of the protein whereas the tryptophans are located on the surface of the protein. Toc34 was aligned with two GTPases, hRas21p and Rap2p, whose structures have been solved (*50*, *51*). In line with the conclusions made for the localization of the tyrosines and tryptophans, the amino acids aligned with the tyrosines were buried and the amino acids aligned with the tryptophans were located on the surface of the proteins (Supporting Information). We therefore conclude that the cytosolic domain of Toc34 folds into a structure similar to that of known GTPases and the expressed protein should be able to function as a receptor for preproteins.

Physiological evidence that Toc34 has folded into a functional protein was obtained from its ability to inhibit import of a preprotein into chloroplasts. Both phosphorylated and nonphosphorylated preSSU are capable of being imported into chloroplasts (Figure 2, lane 1). Addition of GTP or Toc34ΔTM during import reduced the translocation efficiency of the nonphosphorylated preprotein by maximal 50% (lower gel, lanes 2−5). In contrast, import of the

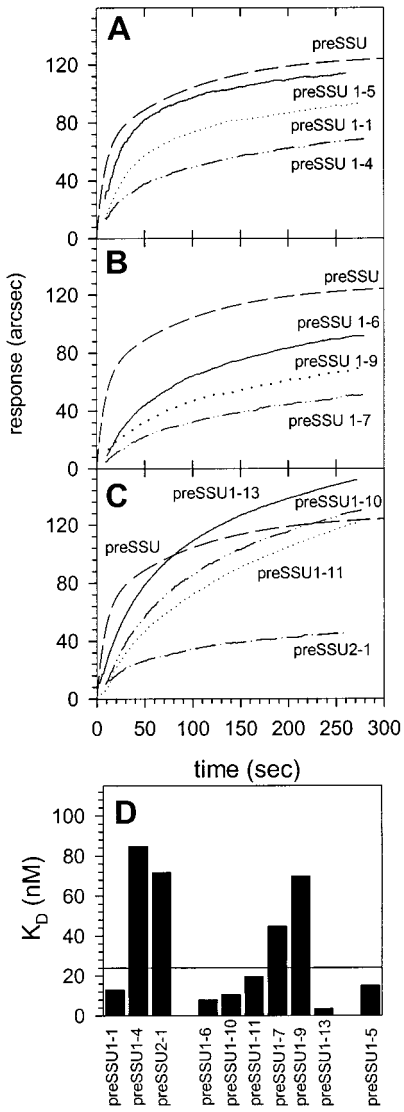

FIGURE 7: Association of wt-preSSU and different mutants with Toc34. (A−C) Toc34ΔTM-6×His (1.16n M) were immobilized. The association of the preSSU mutants to Toc34 was determined in the presence of 0.5 mM GTP. Nomenclature and concentration are given in Table 4 and corresponding curves are labeled. (D) Dissociation constants are sorted by the location of the point mutation.

phosphorylated preprotein is not affected by the addition of GTP or Toc34ΔTM (upper gel, lanes 2−4). However, addition of Toc34 to the translation product prior to import significantly impaired import (upper gel, lane 5). The latter results document a higher affinity of Toc34 for the phosphorylated preprotein. The different effects of Toc34 either preincubated with chloroplasts or with the phosphorylated preprotein protein (upper gel, lanes 4 and 5) might be explained by the interaction of the guidance complex (*45*) with the docking side on the chloroplast surface: a direct transfer of the preprotein from the guidance complex to the pore prevents competition by Toc34ΔTM (upper panel, lane 4). When Toc34 was added to the translation product in the absence of chloroplasts, it effectively competed with the preprotein of the guidance complex and prevented its binding to the Toc complex (upper gel, lane 5). Preloading of Toc34ΔTM with GTP completely abolished the import of both phosphorylated and nonphosphorylated preSSU (lane 6), supporting the earlier finding that Toc34 reveals the highest affinity for preproteins in the presence of GTP (*7*). When GTP was added to the chloroplasts synonymous with the preloading of endogenous Toc34 and Toc159 (lanes 7 and 8), translocation of preSSU was reduced by addition of Toc34ΔTM but not abolished as seen before (lane 6). However, when Toc34ΔTM was added to the preprotein prior to addition of GTP-loaded chloroplasts (lane 7) the import of the nonphosphorylated preprotein was more reduced than the translocation of the phosphorylated preprotein. In the latter case, Toc34ΔTM has to compete for the preprotein−guidance complex and for preprotein−surface receptor interaction. In contrast, in the case of the nonphosphorylated preprotein, Toc34ΔTM only competes for preprotein−surface receptor interaction. When Toc34ΔTM and GTP are given to the chloroplasts (lane 8), the preprotein binds in the same manner to endogenous and added receptor components, resulting in a reduced efficiency of translocation but not in a complete inhibition. Taken together with this, we can demonstrate that Toc34 has a high affinity for the phosphorylated precursor protein in the presence of GTP and is able to compete for protein translocation. Further, the observed difference of import inhibition of phosphorylated and nonphosphorylated preprotein is in line with the presence of a guidance complex in wheat germ lysate (*45*).

The investigation of the interaction of Toc34 with preproteins containing bipartide transit peptides for thylakoid targeting or transit peptides for stromal targeting revealed a high-affinity binding (Figure 4 and Table 2), which is dependent on the presence of GTP (Figures 4 and 5 and Table 2). This suggests that Toc34 recognizes all classes of preproteins. This finding is in line with the observation that chemical amounts of thylakoid-targeted preproteins inhibit import of all classes of preproteins (*54*). In the absence of GTP or GDP the dissociation constant is up to 20-fold higher. The influence of GDP was found to be dependent on the preprotein used (Figure 4 and Table 2). While the interaction of preSSU with Toc34ΔTM was reduced 10-fold in the presence of GDP, the association of preOE33 was only reduced by a factor of 3 when compared to the association in the presence of GTP. Interestingly, the first-order on rate of preSSU and preOE33 was drastically reduced in the presence of GDP compared to first-order on rates in the presence of GTP (Table 2). Therefore, the difference of the dissociation constant of preSSU and preOE33 observed in the presence of GDP is only defined by the dissociation rate of the receptor−preprotein complex. Whereas preSSU will be released from Toc34ΔTM 3 times faster in the presence of GDP than GTP, the speed of complex disassembly of preOE33 and Toc34 is not affected by the GTP to GDP conversion. The reason for the latter finding is not known. However, it could reflect a different mode of transit peptide recognition by Toc34 for preproteins targeted to the thylakoids, such as preOE33. The release of those preproteins containing a bipartite transit peptide is therefore not dependent only on the action of Toc34 itself, as can be proposed for the preproteins containing transit peptides for stromal targeting.

The association of Toc34 is mediated by the transit sequence of the preprotein since Toc34 does not recognize the mature protein (Figure 5C). However, truncation of the mature domain results in reduction of affinity (defined as Gibbs energy change caused by the interaction and given in

Table 3 and Figure 5D). The dissociation constant increases with the amount of amino acids deleted (Table 3). Deletion of the 52 C-terminal amino acids resulted in a minor increase of the dissociation constant in the presence of GTP, almost not affecting the affinity of Toc34ΔTM and preSSU (Table 3). Interestingly, the dissociation constant of preSSUΔ52 in the absence of GTP was in the same range as found for preSSU, namely, $K_D = 140$ nM (data not shown). Deletion of the 67 amino acids already resulted in an increase of the dissociation constant by a factor of 15 (Table 3). The further truncation of the mature region down to two amino acids in His-S-SStp increases the dissociation constant ~230-fold and results in 2-fold lower binding affinity. This is in line with the observation that, with increasing deletion from the C-terminus of the mature domain, the proteins became less active as competitive inhibitors in chloroplast import studies. The IC_{50} value (defined as the concentration of inhibitor required to inhibit 50% of activity) was found to be 6 times higher in the absence of the mature domain than in its presence, whereas deletion of the 52 C-terminal amino acids did not cause a measurable loss in inhibition activity (*33*). This results can be explained by the found affinities of this proteins for the receptor component, Toc34 (Table 3).

Compared to the full-length preSSU, the transit peptide has a dissociation constant 3 orders of magnitude higher than that for the receptor (Figure 3 and Table 3). The further investigation of different regions of the transit peptide revealed that Toc34 recognizes the C-terminal phosphorylatable region of the transit peptide (Figure 6). Even though the affinity of the transit peptide or regions of the transit peptide was found to be reduced, the GTP dependence of this interaction still remained (Figure 6). In line with the experiments on the N- and C-terminus of the transit peptide, only point mutations within the C-terminal portion of the transit sequence decrease the affinity (Figure 7). Since both kinds of mutations, reducing and inducing flexibility, revealed the same effect, we conclude that the transit sequence is already "optimized by nature" in its flexibility for receptor recognition. It is remarkable that Toc34 recognizes specifically the region of the transit peptides, which might form an α-helical structure in hydrophobic environment (Figure 6). A similar result was observed for the recognition of mitochondrial preproteins by Tom20. Even further, Tom20 was able to induce the helical conformation after recognition of the mitochondrial targeting signal (*24*, *25*). Therefore, we hypothesize that Toc34 might induce such structure as well. This can further explain why point mutations disturbing the helix result in a reduction of recognition (Figure 7 and Table 4).

Furthermore, the dissociation constant was 10-fold lower when the C-terminal region was phosphorylated (Table 2), suggesting in vivo a dissociation constant of the interaction of Toc34 and the phosphorylated preSSU of around 2 nM. Interestingly, the dissociation constant of the phosphorylated peptide B1 and Toc34 was only increased 4-fold in the presence of GDP compared to the presence of GTP, and the dissociation constant of the nonphosphorylated peptide was not altered by GTP to GDP conversion. This suggested on one hand that the mature domain has an influence on the ratio of the dissociation constant of Toc34 and preSSU in the presence of GTP or GDP and on the other hand that phosphorylation of the preprotein further sensitizes the interaction of the receptor and the preprotein. A similar influence of phosphorylation was found for nuclear localization signals, where the recognition by the receptor units is either enhanced by phosphorylation of the nuclear localization signal at a CKII site or disturbed by phosphorylation at a cdk/cdc2 site (*55*). Therefore, the difference of the dissociation constants observed for the nonphosphorylated preSSU−Toc34 complex in the presence of GTP and GDP might be even more drastic for the phosphorylated preprotein. This is in line with the earlier observed dissociation constant of 0.1 nM for the association of phosphorylated preSSU and Toc34 (*7*). However, the high affinity and the difference of the GTP/GDP sensitivity suggests an active release process of the preprotein by the receptor.

ACKNOWLEDGMENT

We are grateful to Dr. H. Decker and Dr. N. Hellmann for supervision of the CD experiments.

SUPPORTING INFORMATION AVAILABLE

One color figure showing the proposed location of the aromatic amino acids of Toc34. This information is available free of charge via the Internet at http://pubs.acs.org.

REFERENCES

1. Schleiff, E. (2000) *J. Bioenerg. Biomembr. 32*, 55−66.
2. Schleiff, E., and Soll, J. (2000) *Planta 211*, 449−456.
3. Schnell, D. J., Blobel, G., Keegstra, K., Kessler, F., Ko, K., and Schnell, J. (1997) *Trends Cell Biol. 7*, 303−304.
4. Schnell, D. J., Kessler, F., and Blobel, G. (1994) *Science 266*, 1007−1012.
5. Hinnah, S. C., Hill, K., Wagner, R., Schlicher, T., and Soll, J. (1997) *EMBO J. 16*, 7351−7360.
6. Soll, J., Fischer, I., and Keegstra, K. (1988) *Planta 176*, 488−496.
7. Sveshnikova, N., Soll, J., and Schleiff, E. (2000) *Proc. Natl. Acad. Sci. U.S.A. 97*, 4973−4978.
8. Seedorf, M., Waegemann, K., and Soll, J. (1995) *Plant J. 7*, 401−411.
9. Young, M. E., Keegstra, K., and Froehlich, J. E. (1999) *Plant Physiol. 121*, 237−243.
10. Kouranov, A., and Schnell, D. J. (1997) *J. Cell Biol. 139*, 1677−1685.
11. Gutensohn, M., Schulz, B., Nicolay, P., and Függe, U.-I. (2000) *Plant J. 23*, 771−783.
12. Blobel, G., Walter, P., Chang, C. N., Goldman, B. M., Erickson, A. H., and Lingappa, V. R. (1979) *Symp. Soc. Exp. Biol. 33*, 9−36.
13. von Heijne, G., Steppuhn, J., and Herrmann, R. G. (1989) *Eur. J. Biochem. 180*, 535−545.
14. Bruce, B. D. (2000) *Trends Cell Biol. 10*, 440−447.
15. Neupert, W. (1997) *Annu. Rev. Biochem. 66*, 863−917.
16. Lithgow, T. (2000) *FEBS Lett. 476*, 22−26.
17. Roise, D., Horvath, S. J., Tomich, J. M., Richards, J. H., and Schatz, G. (1986) *EMBO J. 5*, 1327−1334.
18. Epand, R. M., Hui, S. W., Argan, C., Gillespie, L. L., and Shore, G. C. (1986) *J. Biol. Chem. 261*, 10017−10020.
19. Pilon, M., Rietveld, A. G., Weisbeek, P. J., and de Kruijff, B. (1992) *J. Biol. Chem. 267*, 19907−19913.
20. Karslake, C., Piotto, M. E., Pak, Y. M., Weiner, H., and Gorenstein, D. G. (1990) *Biochemistry 29*, 9872−9878.
21. Schleiff, E., Heard, T. S. and Weiner, H. (1999) *FEBS Lett. 461*, 9−12.
22. Hammen, P. K., Gorenstein, D. G., and Weiner, H. (1994) *Biochemistry 33*, 8610−8617.
23. Heard, T. S., and Weiner, H. (1998) *J. Biol. Chem. 273*, 29389−29393.

24. Schleiff, E., and Turnbull, J. L. (1998) *Biochemistry 37*, 13043−13051.
25. Muto, T., Obita, T., Abe, Y., Shodai, T., Endo, T., and Kohda, D. (2001) *J. Mol. Biol. 306*, 137−143.
26. Lancelin, J. M., Bally, I., Arlaud, G. J., Blackledge, M., Gans, P., Stein, M., and Jacquot, J. P. (1994) *FEBS Lett. 343*, 261−266.
27. Krimm, I., Gans, P., Hernandez, J. F., Arlaud, G. J., and Lancelin, J. M. (1999) *Eur. J. Biochem. 265*, 261−266.
28. Wienk, H. L. J., Wechselberger, R., Czisch, M., and de Kruijff, B. (2000) *Biochemistry 39*, 8219−8227.
29. Bruce, B. D. (1998) *Plant Mol. Biol. 38*, 223−246.
30. Pilon, M., Wienk, H., Sips, W., de Swaaf, M., Talboom, I., van't Hoff, R., de Korte-Kool, G., Demel, R., Weisbeek, P., and de Kruijff, B. (1995) *J. Biol. Chem. 270*, 3882−3893.
31. Rensink, W. A., Pilon, M., and Weisbeek, P. (1998) *Plant Physiol. 118*, 691−699.
32. Ivey, R. A., III, Subramanian, C., and Bruce, B. D. (2000) *Plant Physiol. 122*, 1289−1299.
33. Dabney-Smith, C., van den Wijngaard, P. W. J., Treece, Y., Vredenberg, W. J., and Bruce, B. D. (1999) *J. Biol. Chem. 274*, 32351−32359.
34. Subramanian, C., Ivey, R., III, and Bruce, B. D. (2001) *Plant J. 25*, 1−16.
35. Waegemann, K., and Soll, J. (1996) *J. Biol. Chem. 271*, 6545−6554.
36. Pinnaduwage, P., and Bruce, B. D. (1996) *J. Biol. Chem. 271*, 32907−32915.
37. Jones, D. T. (1999) *J. Mol. Biol. 292*, 195−202.
38. Garnier, J., Gibrat, J.-F., and Robson, B. (1996) *Methods Enzymol. 266*, 540−553.
39. Deleage, G., and Roux, B. (1987) *Protein Eng. 4*, 289−294.
40. Rost, B., and Sander, C. (1993) *J. Mol. Biol. 232*, 584−599.
41. King, R. D., and Sternberg, M. J. E. (1996) *Protein Sci. 5*, 2298−2310.
42. Salamov, A. A., and Solovyev, V. V. (1995) *J. Mol. Biol. 247*, 11−15.
43. Frishman, D. A. P. (1996) *Protein Eng. 9*, 133−142.
44. Schleiff, E., and Turnbull, J. T. (1998) *Biochemistry 37*, 13052−13058.
45. May, T., and Soll, J. (2000) *Plant Cell 12*, 53−63.
46. Schleiff, E., Tien, R., Salomon, M., and Soll, J. (2001) *Mol. Biol. Cell 12*, 4090−4102.
47. Monera, O. D., Kay, C. M., and Hodges, R. S. (1994) *Protein Sci. 3*, 1984−1991.
48. Shortle, D. (1989) *J. Biol. Chem. 264*, 5315−5318.
49. Kessler, F., Blobel, G., Patel, H. A., and Schnell, D. J. (1994) *Science 266*, 1035−1039.
50. Pai, E. F., Krengel, U., Petsko, G. A., Goody, R. S., Kabsch, W., and Wittinghofer, A. (1990) *EMBO J. 9*, 2351.
51. Cherfils, J., Menetrey, J., Le Bras, G., Janoueix-Lerose, I., de Gunzburg, J., Garel, J. R., and Auzat, I. (1997) *EMBO J. 16*, 5582−5591.
52. Cush, R., Cronin, J. M., Steward, W. J., Maule, C. H., Molloy, J. O., and Goddard, N. J. (1993) *Biosens. Bioelectron. 8*, 347−353.
53. Chaudhuri, T. K., Arai, M. Terada, T. P, Ikura, T., and Kuwajima, K. (2000) *Biochemistry 39*, 15643−15651.
54. Row, P. E., and Gray, J. C. (2001) *J. Exp. Bot. 52*, 47−56.
55. Jans, D. A., and Hübner, S. (1996) *Phys. Rev. 76*, 651−685.

BI011361+